2012 IEEE International Conference on Power Electronics, Drives and Energy Systems
December16-19, 2012, Bengaluru, India

Synchronization of Variable Speed PMSG Based Wind Energy Conversion System to the Grid with Power Quality Improvement Features

Narsa Reddy Tummuru, Mahesh K. Mishra, *Senior Member, IEEE*, and S. Srinivas, *Member, IEEE*
Department of Electrical Engineering,
Indian Institute of Technology Madras, Chennai, India.
narasaiitm@gmail.com

***Abstract*—This paper presents, grid synchronization of directly driven variable speed permanent magnet synchronous generator (PMSG)-based wind turbine with unbalanced and non liner loads at the point of common coupling (PCC). The machine-side voltage source converter (M-VSC) is controlled by an efficient vector control strategy to extract the maximum power from the fluctuating wind and grid-side voltage source converter (G-VSC) is actively controlled by instantaneous symmetrical components theory, to feed generated active power as well as to supply the harmonics and reactive power demanded by the non-linear and unbalanced load at the PCC, thus enabling the grid to supply only sinusoidal current at unity power factor. A model of directly driven PMSG-based variable speed wind energy conversion system (WECS) is developed and simulated in MATLAB/SIMULIK environment. The effectiveness of proposed control strategies for M-VSC and G-VSC are validated through extensive simulation studies.**

***Index Terms*—Wind Energy conversion, permanent magnet synchronous generator, instantaneous symmetrical components theory.**

I. Introduction

TO have sustainable growth and social progress, it is necessary to meet the energy need by utilizing the renewable energy resources like wind, photo voltaic (PV), biomass, hydro, co-generation,etc. In sustainable energy system, energy conservation and the use of renewable source are the key paradigm. Among renewable energy resources, wind power is today's most rapidly growing renewable energy source. The wind turbine operates either at a fixed or variable speed [1]. In the early stage of wind power development, fixed-speed wind turbines and induction generators were often used in wind farms [2]. But the limitations of such generators, e.g. low efficiency and poor power quality, adversely influence their further applications. With large-scale exploration and integration of wind resources, variable speed wind turbine generators, such as doubly fed induction generators (DFIGs) and permanent magnetic synchronous generators (PMSGs) are emerging as the preferred technology [3]. The variable speed wind turbine with a multipole PMSG and fully controllable voltage source converters (VSCs) is considered to be a promising, but not yet very popular, wind turbine concept. The advantages of PMSG configuration are 1) gearless construction 2) the elimination of a dc excitation system 3) full controllability of the system for maximum wind power extraction and grid interface and 4) ease in accomplishing fault-ride through and grid support. Therefore, the efficiency and reliability of a VSC-based PMSG wind turbine is assessed to be higher than that of a DFIG wind turbine [3], [4].

The control of a variable speed PMSG by a diode rectifier cascaded by a dc chopper is proposed in [5], this system has merits, such as simple construction and low cost. However, it lacks control capability over the generator power factor, which reduces the generator efficiency. Additionally, high harmonic current distortions in the generator windings further degrade the efficiency and produce torque oscillations. In full converter based WECS, vector control and direct torque control are the most commonly used strategies in the generator side. The two strategies have similar dynamic responses and both of them allow separate control of the reactive and active current components (or flux and torque) of the generator. There are many control schemes reported in the literature for control of G-VSC in micro grid application such as synchrounous reference theory, power balance theory, and direct current vector control [1], [3], these algorithms requires complex transformations. Compared to the control strategies mentioned before, the instantaneous symmetrical component based control [6] is simple in formulation, avoids interpretation of instantaneous reactive power and no need of complex transformations. In this paper, the instantaneous symmetrical component theory is extended to control G-VSC in micro grid applications with the following features (i) to regulates the dc-link voltage (ii) to injects the generated wind power into the grid. In addition to this, this control is also utilised to improve power quality issues like (a) compensation of the reactive power, (b) load balancing and (c) current harmonics generated by non-linear loads, if any, at the PCC. This enables the grid to supply only sinusoidal current at unity power factor (UPF). An efficient vector control strategy to M-VSC to synchronize the WECS to grid. The M-VSC controls the generator speed in order to achieve maximum power point tracking (MPPT). The simulation results are provided to validate the active power injection as well as power quality improvement features simultaneously.

This paper is structured as follows. In section II System configuration and modeling of various components are presented. The proposed control strategy for M-VSC and G-

978-1-4673-4508-8/12/$31.00 ©2012 IEEE

VSC is discussed in section III. The design parameters of G-VSC are expalined in section IV. The simulation results are presented in section V. With concluding remarks in section VI.

II. System Configuration and Modeling

The system under consideration employs PMSG-based variable speed WECS consisting of two back-to-back voltage source converters with a common dc-link. The description of variable speed WECS is shown in Fig. 1. The system with their important characteristics are discussed below.

A. Aerodynamic Model

The wind turbine extracts power from wind and then converts it into mechanical power. The amount of mechanical power from wind turbine is given [7] by,

$$P_m = \frac{\rho \pi r^2 V_w^3 C_p(\lambda, \theta)}{2} \tag{1}$$

where ρ is the air density, r is the radius of circular swept area of rotor blades, V_w is the wind velocity, λ is tip speed ratio, and θ is the pitch angle. The wind power captured by wind turbine depends on its power co-efficient $C_p(\lambda, \theta)$ which is given by the relation,

$$C_p(\lambda, \theta) = \frac{P_{turbine}}{P_{wind}}. \tag{2}$$

For a given turbine, $C_p(\lambda, \theta)$ is not always constant. $C_p(\lambda, \theta)$ is a function of the tip speed ratio (λ) and the pitch angle (θ). The tip speed ratio is given as

$$\lambda = \frac{W_r\, r}{V_w} \tag{3}$$

from the above equations, different wind speeds will require the optimal values of tip speed (λ_{opt}) and pitch angle (θ) to achieve a optimum $C_{p,opt}$ and therefore giving the highest power output at all available wind speeds. figure

B. Dynamic model of PMSG

Recently the PMSG has been gaining a lot of attention for WECS because of compact size, higher power density, reduced losses, high reliability and robustness. The dynamic model of PMSG can be represented in a rotating reference frame with the help of following equations [8].

$$v_q = R_s i_q + L_q \frac{di_q}{dt} + w_r L_d i_d + w_r \lambda_m \tag{4}$$

$$v_d = R_s i_d + L_d \frac{di_d}{dt} - w_r L_q i_q \tag{5}$$

$$T_e = \left(\frac{3}{2}\right)\left(\frac{P}{2}\right)\lambda_m i_q \tag{6}$$

where P is the number of poles, λ_m is magnetic flux, L_d is direct-axis inductance, L_q is quadrature-axis inductance, R_s is resistance of stator, and w_r is rotor speed of the generator.

C. Power Electronic Interface

Several types of power electronic interfaces have been investigated for variable speed wind turbines [9]. The system under consideration consists of two back-to-back fully controlled voltage source converters decoupled by a dc-link. The converters have been realised by using six switches for each converter. Since PMSG is connected to the grid through an ac/dc/ac system, the power generated P_{gen} by PMSG is first transferred to dc-link and then from dc-link to grid.

III. Control Strategy for M-VSC

The control strategies for M-VSC and G-VSC are discussed in the following sections.

A. M-VSC control approach

The complete Generator side control scheme is shown in Fig. 3.

1) Vector Control: In the vector control of PMSG, the rotor flux rotates at speed (w_r) and its position angle(θ)can be obtained with respect to an arbitrary reference axis as

$$\theta = \int w_r dt \tag{7}$$

The d-axis reference current component can be set to zero in order to obtain maximum torque at minimum current and therefore to minimise the resistive losses in the generator. Using equation (6) the developed torque is given by

$$T_e = K_t i_q \tag{8}$$

where

$$K_t = \left(\frac{3}{2}\right)\left(\frac{P}{2}\right)\lambda_m$$

Hence, from equation (8) it is evident that the vector control action forces the PMSG operation to that of an equivalent separately excited dc machine.

a) Outer Speed loop design: The PMSG vector control has two control loops (i) inner current control loop and (ii) outer speed control loop. The three phase reference currents are generated by outer speed control loop. The outer speed control loop requires actual rotor position and its speed. The main objective of this control is to track speed command. The speed error is processed by the speed controller to obtain torque command of the generator, which is expressed as

$$T_e^* = \left(K_{pw} + \frac{K_{iw}}{s}\right)(w_r^* - w_r) \tag{9}$$

The quadrature-axis reference component of current of generator is computed using (6), and is given as following.

$$i_q^* = \frac{4}{3}\left(\frac{T_e^*}{P\lambda_m}\right) \tag{10}$$

Where Kp_w and Ki_w are the proportional and integral constants of generator outer speed loop which are designed as follows.

The equations (4), (5), and (6) are needed for the speed controller design. The stator time constant of the machine in

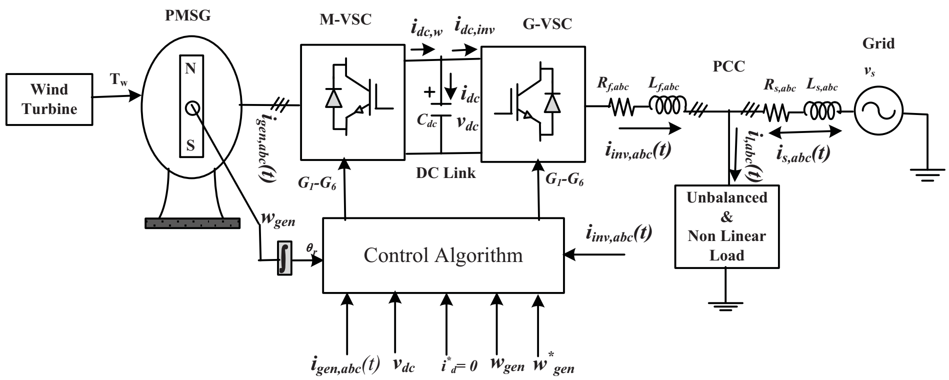

Fig. 1. Block diagram representation of variable speed PMSG based WECS.

this paper is such that the current controller switching delay can be neglected. In addition, equations (4) and (5) describe the stator current dynamics. If the stator time constant is much smaller than the mechanical time constant of the machine, then it can be assumed that the actual current assumes the commanded value in negligible time when compared to the mechanical time constant of the machine. The design of the

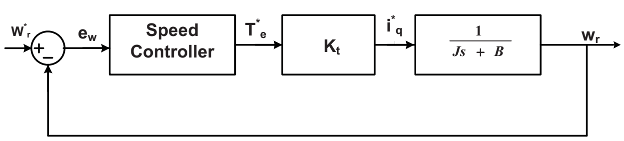

Fig. 2. Outer speed control loop of PMSG.

speed loop assumes that the current loop is much faster than speed loop, allowing to reduce the system block diagram by considering the current loop to be of unity gain as shown in Fig. 2. The loop gain transfer function of the outer loop is,

$$G_{(s)}H_{(s)} = \frac{k_t(K_{pw}s + K_{iw})}{s(Js + B)}. \tag{11}$$

The crossover frequency of the outer speed loop is chosen in such a way that, it is smaller than the current loop. To satisfy dynamic response characteristics the phase margin (φ_m) should be greater than 45^o, preferably close to 60^o. Knowing the generator parameters and phase margin, the K_{pw} and K_{iw} gains can be obtained for the outer speed loop controller using equations (12) and (13) as given below.

$$\left|G_{(s)}H_{(s)}\right| = \left|\frac{k_t(K_{pw}s + K_{iw})}{s(Js + B)}\right|_{s=jw_{gc}} = 1 \tag{12}$$

$$\angle G_{(s)}H_{(s)} = \angle\frac{k_t(K_{pw}s + K_{iw})}{s(Js + B)} = 180^o + \varphi_m \tag{13}$$

B. G-VSC Control approach

The G-VSC control scheme is shown in Fig. 4. The G-VSC control is used to regulate dc-link voltage so that the power balance can be maintained under both fluctuating wind and grid disturbances. The load may consist of three components,

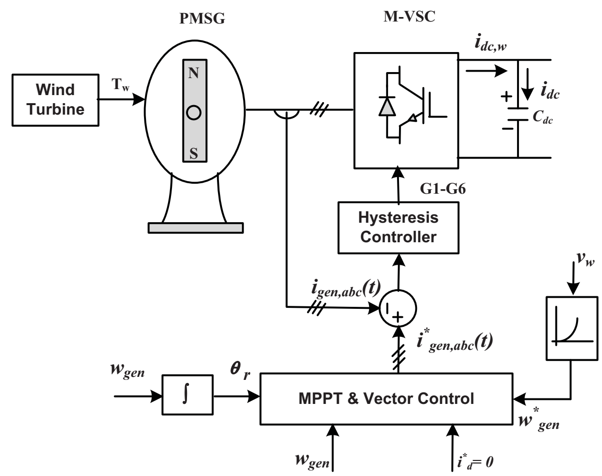

Fig. 3. Block diagram of generator side control.

the fundamental active component (in-phase component), the reactive component (quadrature component) and the harmonic currents (or harmonic reactive component). Therefore, if the G-VSC supplies the active current proportional to generated wind power, the reactive and harmonic currents of load, then the grid needs only to supply active current to the load at PCC.

In this work, the reference currents for G-VSC are generated using instantaneous symmetrical component theory [6]. The purpose of the proposed scheme is to generate the three reference current waveforms in proportion to the wind power and compensation requorement, In three-phase four-wire system or three phase three-wire with ground, three phase currents are independent. Thus, three independent equations are required to generate these currents. The extraction of reference currents is given as follows,

Condition 1 : The supply current must be balanced.

$$i_{sa} + i_{sb} + i_{sc} = 0\,. \tag{14}$$

Condition 2 : The desired power factor of the source can be set explicitly, to have a predefined power factor from the source, the relationship between the angle of $\vec{v}_{sa1}$ and $\vec{i}_{sa1}$ is given

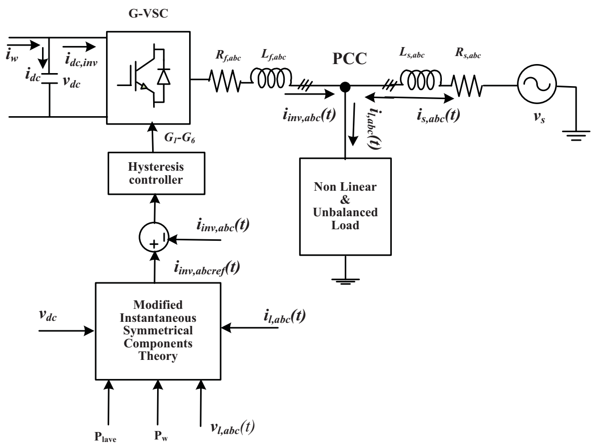

Fig. 4. Block diagram of grid side control.

as following.

$$\angle \vec{v}_{sa1} \; = \; \angle \vec{i}_{sa1} + \phi . \tag{15}$$

Where ϕ is desired phase angle between $\vec{v}_{sa1}$ and $\vec{i}_{sa1}$.

Condition 3: The source should supply or absorb the net average power $(P_s = P_{lavg} - P_{\mu s} + P_{loss})$.

$$P_s = v_{sa}\, i_{sa} + v_{sb}\, i_{sb} + v_{sc}\, i_{sc} = P_{lavg} - P_{\mu s} + P_{loss}. \tag{16}$$

By solving equations (14), (15) and (16), the G-VSC reference currents are obtained as follows,

$$\begin{aligned} i^*_{inv,a} &= i_{la} - \frac{v_{sa} + \beta(v_{sb} - v_{sc})}{\Delta}(P_{lavg} - P_{\mu s} + P_{loss}) \\ i^*_{inv,b} &= i_{lb} - \frac{v_{sb} + \beta(v_{sc} - v_{sa})}{\Delta}(P_{lavg} - P_{\mu s} + P_{loss}) \\ i^*_{inv,c} &= i_{la} - \frac{v_{sc} + \beta(v_{sa} - v_{sb})}{\Delta}(P_{lavg} - P_{\mu s} + P_{loss}) \end{aligned} \tag{17}$$

where,

$$\Delta = \sum_{j=a,b,c} v^2_{sj}, \beta = tan\varphi/\sqrt{3} = \frac{Q_s}{P_s\,\sqrt{3}} .$$

Where $Q_s = Q_l - Q_{\mu s}$, and by substituting $\beta\, P_s = \frac{Q_s}{\sqrt{3}}$ into the equation (17), the modified G-VSC reference current equations in terms of active and reactive components are

$$\begin{aligned} i^*_{inv,a} &= i_{la} - \frac{v_{sa}\, P_s}{\sum_{j=a,b,c} v^2_{sj}} - \frac{(v_{sb} - v_{sc})\, Q_s}{\sum_{j=a,b,c} v^2_{sj}\sqrt{3}} \\ i^*_{inv,b} &= i_{lb} - \frac{v_{sb}\, P_s}{\sum_{j=a,b,c} v^2_{sj}} - \frac{(v_{sc} - v_{sa})\, Q_s}{\sum_{j=a,b,c} v^2_{sj}\sqrt{3}} \\ i^*_{inv,c} &= i_{lc} - \frac{v_{sc}\, P_s}{\sum_{j=a,b,c} v^2_{sj}} - \frac{(v_{sa} - v_{sb})\, Q_s}{\sum_{j=a,b,c} v^2_{sj}\sqrt{3}} \end{aligned} \tag{18}$$

Where $P_{\mu s}$, P_{lavg}, and Q_l are the available microsource power, average load power, and load reactive power respectively. P_{loss} denotes the switching losses and ohmic losses in actual compensator and it is generated using a capacitor voltage PI controller. The term P_{lavg} is obtained using a moving average filter of one cycle window of time T in seconds.

TABLE I
SYSTEM PARAMETERS

System Quantities	Values
System voltages	$150V$ peak phase to neutral, $50Hz$
Linear Load	Z_{la} = $50 + j1.57$ Ω, Z_{lb} = $45 + j3.14$ Ω, Z_{lc} = $40 + j4.71$ Ω
Non-Linear Load	Three phase full bridge rectifier load feeding a R-L load of 44Ω-$3mH$
G-VSC parameters	C_{dc}=660μF, V_{dcref}=600V, L_f= $5mH$, R_f= 0.1Ω
PI controller gains	K_p=2, K_i=0.5
Hysteresis band	$0.25A$

IV. Design of G-VSC parameters

The parameters of the G-VSC need to designed carefully for better tracking performance. The important parameters that need to be taken into consideration while design are (i) DC link voltage (V_{dc}), (ii) DC link capacitor (C_{dc}) value, (iii) interfacing inductor (L_f),(iv) switching frequency (f_{sw}). A detailed design procedure for these parameters is given in [10], based on the the following equations the above parameters of G-VSC are chosen and the system parameters are given in Table I.

$$C_{dc} = \frac{(2X - X/2)nT}{(1.8V_m)^2 - (1.4V_m)^2} \tag{19}$$

where, V_m is the peak value of the source voltage, X is the kVA rating of the system, n is number of cycles and T time period of each cycle. The interfacing inductance is given by

$$L_f = \frac{1.6V_m}{4hf_{swmax}} \tag{20}$$

In this paper the switching commands for the G-VSC and M-VSC switches are generated using hysteresis band current control method.

V. Simulation Studies

The proposed control strategy for PMSG-based variable speed WECS is simulated using MATLAB/SIMULINK under fluctuating wind conditions. In order to simulate the transient response of the proposed control system, wind speed is assumed to have a step-down from 14 to 11 m/s at 0.4 s, and a step-up from 11 to 14 m/s at 0.9 s. As a result, the reference speed for generator is changed accordingly and the power flow between the G-VSC, grid and load is also varied under above the operating conditions.

A. Performance of vector controlled PMSG with wind fluctuations

The dynamic performance of proposed control strategy with different wind conditions are shown in Fig. 5. A variable input torque in proportion to wind speed is applied to PMSG and accordingly reference speed is calculated using the MPPT

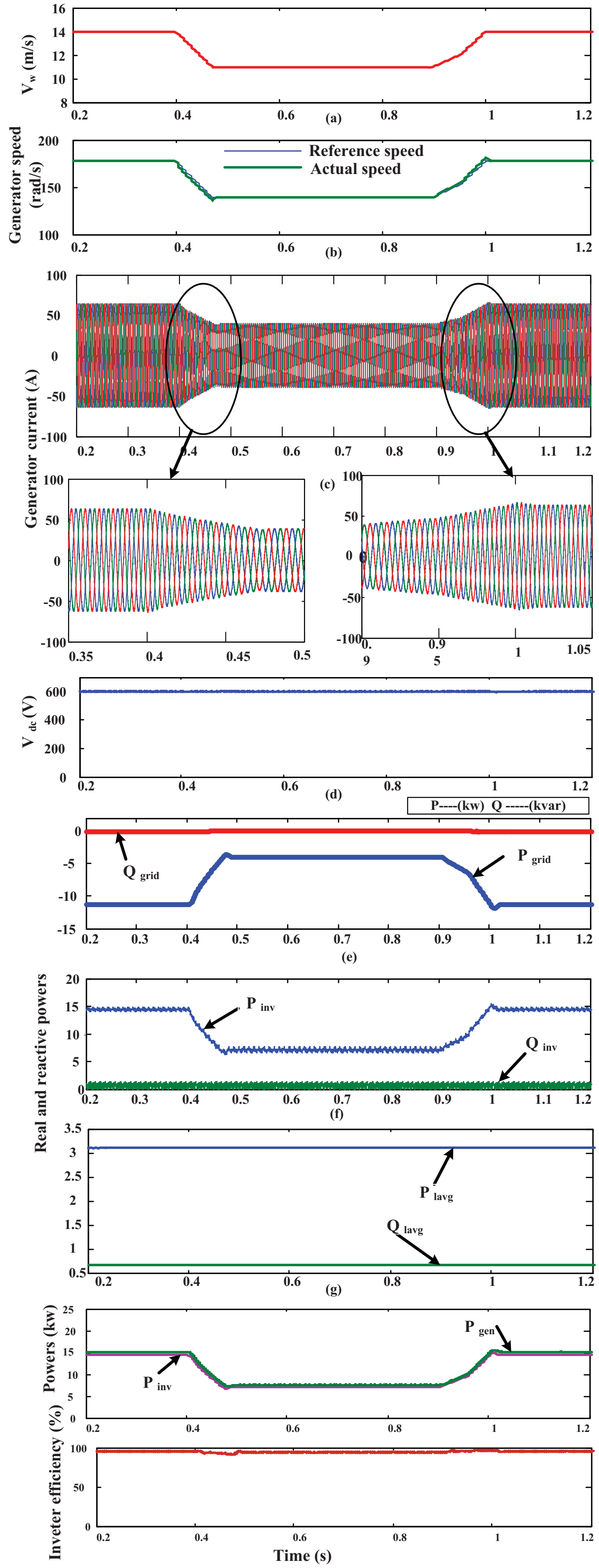

Fig. 5. Simulation results: performance of proposed control approach (a) wind speed (b) Generator actual and reference speeds (c) Generator current (d) Dc-link voltage (e) Grid active and reactive powers (f) G-VSC injected active and reactive powers (g) load average active,reactive powers and inverter efficiency.

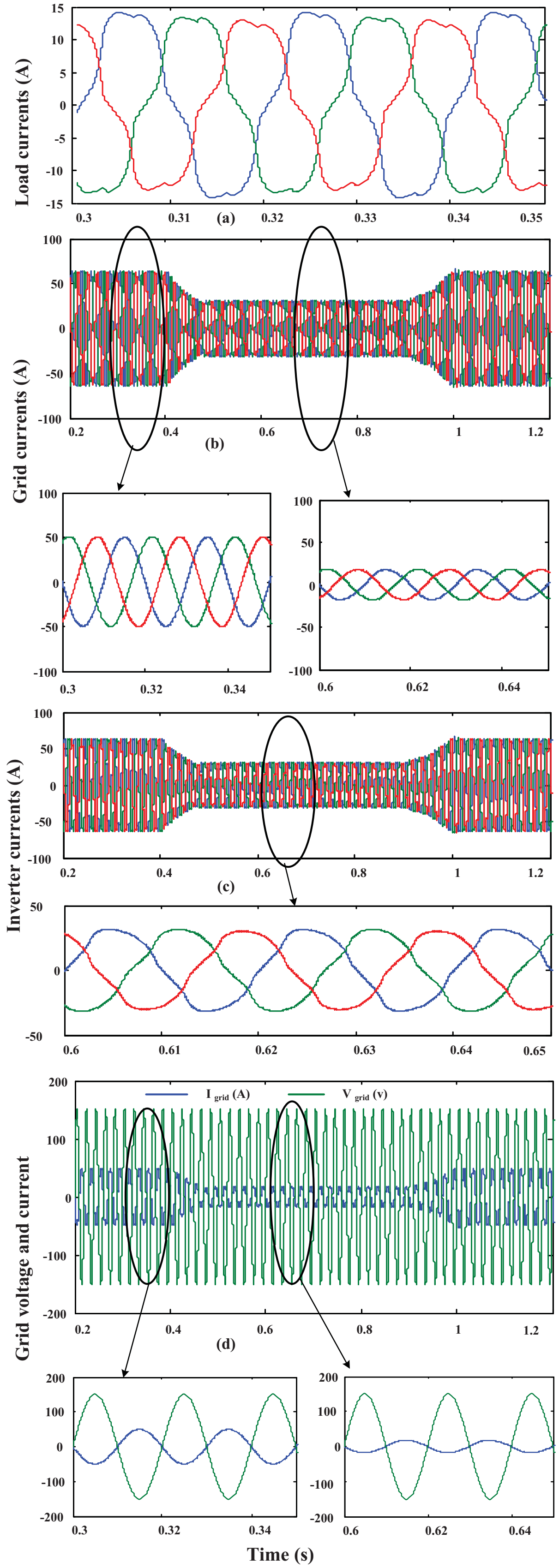

Fig. 6. Simulation results using proposed control approach: (a) Load currents (b) Grid currents (c) G-VSC currents (d) Grid voltage and current in phase-a.

TABLE II
MAXIMUM POWER TRACKING PERFORMANCE

Time (s)	V_w (m/s)	W_{ref} (rad/s)	W_r (rad/s)	P_{max} (kw)
0.2 − 0.4	14	177	177	14.9
0.4 − 0.9	11	147	147	7
0.9 − 1.2	14	177	177	14.9

algorithm. The objective of vector control approach is that, the speed of generator should track the reference speed closely. The tracking performance of the MPPT algorithm is shown in Fig. 5(a)-(c) and important values are given in Table II for the above operating wind conditions. The actual and reference speed with reference to wind fluctuations are shown in Fig. 5(b). From these simulation results it can be concluded that, the outer speed controller tracks the speed of generator very close to the reference value which in turn acheives the MPPT feature.

B. Performance of grid side controller with wind fluctuations

The G-VSC is actively controlled to inject the generated active power as well as to compensate the harmonic and reactive power demanded by the unbalanced and non-linear load at PCC, such that the current drawn from grid is purely sinusoidal at UPF, which is shown in Fig. 6(d) and also to regulate the dc link voltage. The dynamic compensation performance of G-VSC is shown in the Figs. 6(b)-(d) for fluctuating wind and given load conditions. At time t= 0.2-0.4 s, the wind speed is 14 m/s, in this case the G-VSC starts injecting the current which is the sum of harmonic component, reactive component of unbalanced and non-linear load and active component in proportion to the generated wind power as shown in Fig. 6(c), and the corresponding variations in the grid current aganist grid voltage is shown in the Fig. 6(d). The active power supplied by the inveter (15 kw at $V_w = 14$ m/s) is greater than the load power demand (3.1 kw), the surplus power (11.9 kw) is fed into the AC mains. At t=0.4 s, the wind speed starts decreasing and settles to 11 m/s, in this case also the power injected by the G-VSC (7 kw) is greater than load power demand (3.1 kw), the remaining power (3.9 kw) is absorbed by the grid. At t=0.9 s, the wind speed stats increasing and reaches to the beginning state and these dynamics of power flows are shown in the Figs. 6(e)-(g). The dc-link voltage is maintained at a constant level of 600 V irrespective of wind fluctuations.

VI. CONCLUSIONS

The performance of PMSG-based variable speed WECS has been demonstrated with an application of instantaneous symmetrical components theroy to G-VSC and efficient vector control strategy to M-VSC under varying wind conditions. The G-VSC is able to inject the generated power into the grid alongwith harmonic and reactive power compensation of unbalanced non-linear load at the PCC simultaneously. The system works satisfactorily under dynamic conditions. The simulation results under a unbalanced non-linear load with

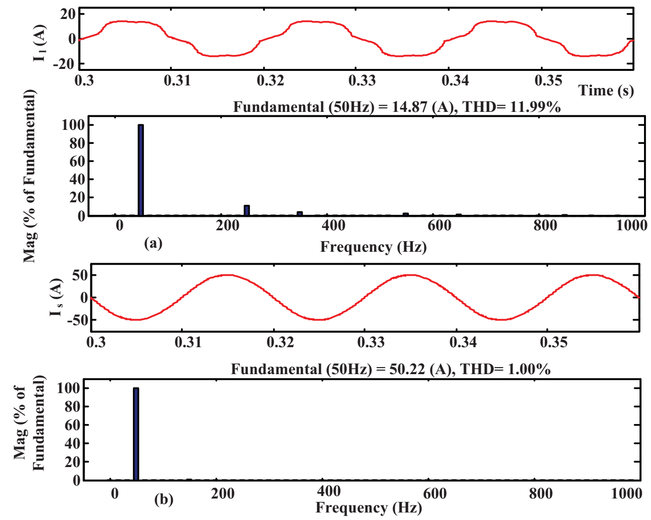

Fig. 7. Simulation results: performance of proposed control approach (a) THD of load currents (b) THD of grid currents

current THD of 12% confirm that the G-VSC can effectively inject the generated active power along with power quality improvement features and thus, it maintains a sinusoidal and UPF current at the grid side with THD of 1%.

REFERENCES

[1] S. Li, T. Haskew, R. Swatloski, and W. Gathings, “Optimal and direct-current vector control of direct-driven pmsg wind turbines,” *Power Electronics, IEEE Transactions on*, vol. 27, no. 5, pp. 2325 –2337, may 2012.

[2] M. Haque, M. Negnevitsky, and K. Muttaqi, “A novel control strategy for a variable speed wind turbine with a permanent magnet synchronous generator,” in *Industry Applications Society Annual Meeting, 2008. IAS ’08. IEEE*, oct. 2008, pp. 1 –8.

[3] S. Zhang, K.-J. Tseng, D. Vilathgamuwa, T. Nguyen, and X.-Y. Wang, “Design of a robust grid interface system for pmsg-based wind turbine generators,” *Industrial Electronics, IEEE Transactions on*, vol. 58, no. 1, pp. 316 –328, jan. 2011.

[4] M. Singh and A. Chandra, “Application of adaptive network-based fuzzy inference system for sensorless control of pmsg-based wind turbine with nonlinear-load-compensation capabilities,” *Power Electronics, IEEE Transactions on*, vol. 26, no. 1, pp. 165 –175, jan. 2011.

[5] H. Geng, G. Yang, D. Xu, and B. Wu, “Unified power control for pmsg-based wecs operating under different grid conditions,” *Energy Conversion, IEEE Transactions on*, vol. 26, no. 3, pp. 822 –830, sept. 2011.

[6] A. Ghosh and A. Joshi, “A new approach to load balancing and power factor correction in power distribution system,” *IEEE Transactions on Power Delivery*, vol. 15, no. 1, pp. 417 –422, Jan. 2000.

[7] M. Chinchilla, S. Arnaltes, and J. Burgos, “Control of permanent-magnet generators applied to variable-speed wind-energy systems connected to the grid,” *Energy Conversion, IEEE Transactions on*, vol. 21, no. 1, pp. 130 – 135, march 2006.

[8] P. Pillay and R. Krishnan, “Control characteristics and speed controller design for a high performance permanent magnet synchronous motor drive,” *Power Electronics, IEEE Transactions on*, vol. 5, no. 2, pp. 151 –159, apr 1990.

[9] F. Blaabjerg, Z. Chen, and S. Kjaer, “Power electronics as efficient interface in dispersed power generation systems,” *Power Electronics, IEEE Transactions on*, vol. 19, no. 5, pp. 1184 – 1194, sept. 2004.

[10] Mahesh K. Mishra and K. Karthikeyan, “Design and analysis of voltage source inverter for active compensators to compensate unbalanced and non-linear loads,” in *Power Engineering Conference, 2007. IPEC 2007. International*, 2007, pp. 649 –654.